Mapping Interaction Forces with the Atomic Force Microscope

Manfred Radmacher, Jason P. Cleveland, Monika Fritz,* Helen G. Hansma, and Paul K. Hansma
Physics Department and *Marine Science Institute, University of California, Santa Barbara, California 83106 USA

ABSTRACT Force curves were recorded as the sample was raster-scanned under the tip. This opens new opportunities for imaging with the atomic force microscope: several characteristics of the samples can be measured simultaneously, for example, topography, adhesion forces, elasticity, van der Waals, and electrostatic interactions. The new opportunities are illustrated by images of several characteristics of thin metal films, aggregates of lysozyme, and single molecules of DNA.

INTRODUCTION

Understanding and controlling interaction forces in atomic force microscopy (AFM) (Binnig et al., 1986; Drake et al., 1989; Rugar and Hansma, 1990) has long been recognized as important (Weisenhorn et al., 1989; Burnham and Colton, 1989; Weisenhorn et al., 1992; Burnham et al., 1991). It is increasingly important as more delicate samples like adsorbed proteins (Egger et al., 1990), Langmuir-Blodgett films (Garnaes et al., 1992; Radmacher et al., 1992), membrane patches (Hoh et al., 1991), and live cells (Keller et al., 1992; Henderson et al., 1992; Häberle et al., 1992; Fritz et al., 1994b; Fritz et al., 1994a) are imaged. A better understanding of these forces has pushed the AFM from a simple, high resolution profilometer to a tool for measuring and imaging a variety of sample properties like local friction (Marti et al., 1990) and elasticity (Radmacher et al., 1993; Baselt et al., 1993). Recently, it was demonstrated that force curves not only contain information about adhesion forces (Hoh et al., 1992), van der Waals forces (Hartmann, 1991), or electrostatic forces (Butt, 1991), but also more complicated properties like elasticity (Tao et al., 1992; Weisenhorn et al., 1993) and lateral forces (Hoh and Engel, 1993). The demonstration that interaction forces can be measured with atomic resolution (Ohnesorge and Binnig, 1993) makes the idea of mapping forces very promising (Mizes et al., 1991; Baselt and Baldeschwieler, 1994). In this paper, we combine the vast information content of force curves with the ability of the AFM to raster-scan the sample with high precision. We record a complete set of force curves and demonstrate how images showing surface topography, adhesion forces, and other properties of the sample can be extracted out of these data sets.

MATERIALS AND METHODS

Two types of thin metal films on different substrates were prepared: nickel on freshly cleaved mica and chromium on glass. These films were evaporated in a home-built thermal evaporator. The average thickness of the nickel deposited was 10 nm, resulting in small isolated islands of nickel on the mica. Chromium was evaporated on a microscope cover slide after a suspension of latex beads (Sigma Chemical Co., St. Louis, MO; radius 450 nm) was air-dried on it. The latex beads shadowed the substrate during evaporation so that the glass was not covered everywhere. Ultrasonication removed the latex beads, resulting in a sample that was only partially covered by chromium.

Lysozyme (from Chicken egg white, purchased at Sigma) was dissolved in a buffer containing 66 mM KH_2PO_4 (pH 6.4) to a concentration of 0.1 mg/ml and adsorbed on freshly cleaved mica. After incubation for 20 min, the buffer was exchanged against a buffer containing 10 mM KH_2PO_4 (pH 6.4). This procedure resulted in relatively stable aggregates of lysozyme that could be imaged easily by AFM. The details and the influence of the buffer composition on whether single molecules or aggregates will adsorb on glass will be discussed elsewhere (Radmacher et al., 1994, in press).

Bluescript plasmid DNA (Stratagene, La Jolla, CA) was dissolved in a buffer containing 0.4 mM HEPES and 0.1 mM $MgCl_2$ (pH 7.6) and adsorbed on freshly cleaved mica. The sample was rinsed with pure water (Milli-Q quality, Millipore, Burlington, MA) and dried for 10 min or longer in vacuum over P_2O_5. It was then imaged in water in the AFM (Hansma et al., 1993; Bezanilla et al., 1993).

Two different kinds of tips were used: homemade electron beam deposited tips (Keller and Chih-Chung, 1992; Hansma et al., 1992) (for the DNA images) and commercially available sharpened silicon nitride tips (Akamine et al., 1990) (Nanoprobes, Digital Instruments, Santa Barbara, CA) (for all other images). The force constants of the levers used was not measured. Therefore, typical values for the wafers were taken. It is known that the force constants vary greatly from wafer to wafer, but vary by less than a factor of two on one wafer (Cleveland et al., 1993).

All measurements were made in buffer, to eliminate strong capillary forces, which are usually present while imaging in air.

Force curve images were recorded using modified Nanoscope II electronics (Digital Instruments). The Nanoscope itself was only used for generating the scan voltages in the x and y directions. The z-signal of the piezo was driven by analog electronics using a function generator (Model 184, Wavetec, San Diego, CA) biased by a high precision DC power supply (Model 6116 A, Hewlett Packard, Santa Clara, CA). The data were recorded on a separate computer (Macintosh Quadra 840 AV, Apple Computers, Cupertino, CA), equipped with a data acquisition board (MacAdios II, GWI Instruments, Sommerville, MA), and controlled by custom software. This program also recorded the scan voltages generated by the Nanoscope so that the data could be split into lines and pixels corresponding to the lateral movement of the piezo after acquisition. The data were rearranged in several ways (see below) and exported to an image analysis program (NIH-Image by Wayne Rasband, National Institutes of Health, Bethesda, MD). The electronics could be switched back, so that the z-voltage was controlled by the Nanoscope again, thus making it possible to acquire conventional topography AFM images.

Typical imaging parameters were the following: force curves were swept at about 70–100 Hz with amplitudes of several hundred nanometers. The approach and the retract curves were sampled at 100 points each. Lateral scanning was performed at about 0.1 Hz scan rate. Typically, only every third force curve was recorded, resulting in 25 force

Received for publication 3 January 1994 and in final form 7 March 1994.
Address reprint requests to Manfred Radmacher, Department of Physics, University of California, Santa Barbara, CA 93106. Tel.: 805-893-3999; Fax: 805-893-8315; E-mail: manfred@physics.ucsb.edu.

0006-3495/94/06/2159/07 $2.00

curves per second, or about 120 force curves per scan line. Because data were recorded for the trace and retrace scan of each lateral scan line and typically 100 lines per image were recorded, a complete data set consisted of 24,000 force curves.

Display of data

There are two common methods of data measurement and presentation in normal AFM. One is the force curve. Here, the x and y voltages are held constant, z is ramped, and the cantilever deflection is measured as a function of z (see Fig. 2). These data are usually displayed in a one-dimensional graph of cantilever deflection versus z. In these graphs, the sloped part of the curve corresponds to heights where the tip is in contact with the surface, the horizontal part of the curve to heights where the tip is not in contact with the surface. A simple transformation (Burnham et al., 1991) easily converts this to the force experienced by the tip as a function of the distance above the sample. The other method is an AFM image. Here, a single height (either the sample height required to keep the deflection of the lever constant, or the deflection of the lever itself) is generated for each of many lateral sample positions (usually a square array). This data then defines a three-dimensional surface that can be visualized using color or gray scale to represent the z data in a two-dimensional image, or using a two-dimensional rendering of the three-dimensional surface.

In the present work, we recorded force curves at each of many lateral sample positions, creating a map of cantilever deflection as a function of sample position in three dimensions. In fact, two separate maps, one for approach and one for retract, are recorded. Data sets of this type are inherently three-dimensional and cannot be visualized easily.

One method of presenting the data is to display a set of force curves as a function of the position as in Figs. 3 and 5. All of the force curves of one scan line are stacked one behind the other, generating a surface we have named a force curve relief. In Fig. 3, two such reliefs, one for approach and one for retract, are displayed using a three-dimensional reconstruction algorithm. This algorithm uses a viewer position and a light source position for calculating the amount of light reflected from each spot of the relief. The side view of these reliefs corresponds to one force curve, but displayed upside down relative to the curves commonly displayed. The plateau in the back of each relief corresponds to the noncontact part of each force curve, the slope in the front to the contact region. The edge of the plateau is the point of contact of every force curve, so the shape of this edge resembles the topography (see Fig. 5).

A different approach is needed for displaying real two-dimensional images, where the position in the image corresponds to the position on the sample and the gray scale at that position corresponds to some measured quantity at that position. In AFM images like Fig. 1 *a*, this quantity is the height. There are several quantities that can be extracted out of the force curve data. One is the z-position of the point of contact. This will result in a height image (Fig. 1 *b*). We defined the point of contact as the intersection of the contact region of the force curve and the noncontact region of the force curve (see Fig. 2 *A*). With this definition, the point of contact is that height, where the tip would have touched the sample, if there is no attractive force resulting in a mechanical instability so that the tip jumps to the sample. This definition makes the point of contact independent of the long range attractive forces and reveals a measure for the topography of the sample. Another quantity is the height of the jump to contact. The jump to contact occurs at that sample position at which the attractive gradient of the force becomes larger than the force constant of the cantilever spring. Therefore, the height of the jump to contact shows how long ranged the attractive forces between tip and sample are. Usually, there is a large hysteresis during retract, which is due to mechanical properties of the cantilever-sample system and adhesion forces. The hysteresis can be measured by its height (in units of force) and its width (in units of nm). Normally, these two numbers are proportional (related by the force constant of the cantilever), but they can be different, for instance, in cases where there are soft adsorbed layers on the sample. These are only the most straightforward quantities to be extracted from force curves. Other quantities like elasticity, electrostatic forces, and lateral forces could also be extracted, as described by other groups (Tao et al., 1992; Weisenhorn et al., 1993; Butt, 1991; Hoh and Engel, 1993). Another example is the elastic response of proteins, which will be discussed elsewhere (Radmacher et al., 1994, in press).

Another more abstract way of thinking and handling our data is the following: we actually have recorded the cantilever deflection or the force as a function of all three space coordinates x, y, and z. So we have measured a scalar function $F(x, y, z)$. We can visualize subsets of the data set by reducing the dimensionality of the data so that it can be displayed as a line or surface. For instance, a one-dimensional slice through this volume in the z direction is just a familiar force curve. A two-dimensional slice in the x-y plane (in the contact region) contains the same data as a constant height AFM image, and a constant force image is an approximation (limited by feedback response) of a two-dimensional constant force surface through the data.

RESULTS

In Fig. 1, images of the thin nickel film evaporated onto a freshly cleaved mica are shown. The average film thickness was 10 nm, resulting in a sample with small separate islands of nickel. Fig. 1 *a* shows the AFM image of this sample before the force image was recorded. Note the streaky features on top of several Ni particles, presumably due to some adsorbed contaminant (see *arrow* in Fig. 1 *a*). Fig. 1 *b* shows the height profiles reconstructed from the force curves. In this figure, the point of contact of the force curve, following the previous definition, is shown. Please note the good congruence between the normal AFM images (Fig. 1 *a*) and the reconstructed data (Fig. 1 *b*). There was also excellent congruence between the images extracted out of the force curve data acquired during trace and retrace. Fig. 1 *c* shows the height of the jump to contact of the force curves. The size of the hysteresis during retract of the force curve is coded in two sets of images: Fig. 1 *d* shows the height of this hysteresis, and Fig. 1 *e* show the width of this hysteresis. Normally, the images of the width and the height of this hysteresis should look similar. However, this is not true in cases where some soft contaminant layer is adsorbed on top of the Ni particles. To make this point clearer, Fig. 2 shows several force curves out of the same data set as in Fig. 1 at three different spots on the sample: Fig. 2 *A* on top of the contaminated particle (see the arrow in Fig. 1 *a*), Fig. 2 *B* on the mica between the Ni islands, and Fig. 2 *C* on an uncontaminated Ni island. Note that the adhesion force on the Ni is usually smaller than on mica, but becomes huge on the contaminant layer. Also, there is no clear jump off visible on the contaminant (Fig. 2 *A*), suggesting some wetting like process (see Discussion).

Fig. 3 shows the reconstruction of one complete line of force curves. The force curves (like in Fig. 2) of one scanning line are stacked one behind the other, building a three-dimensional structure. This structure is displayed using an elaborated computer algorithm, which calculates a 3D reconstruction out of these data. In Fig. 3 *a*, the force curves during approach are shown. Mainly, the topography is visible as sliding back and forth of the contact point. There are two nickel particles crossed in this scan line (see *arrows* in Fig. 3 *a*). Fig. 3 *b* shows the force curves during retract. Note the

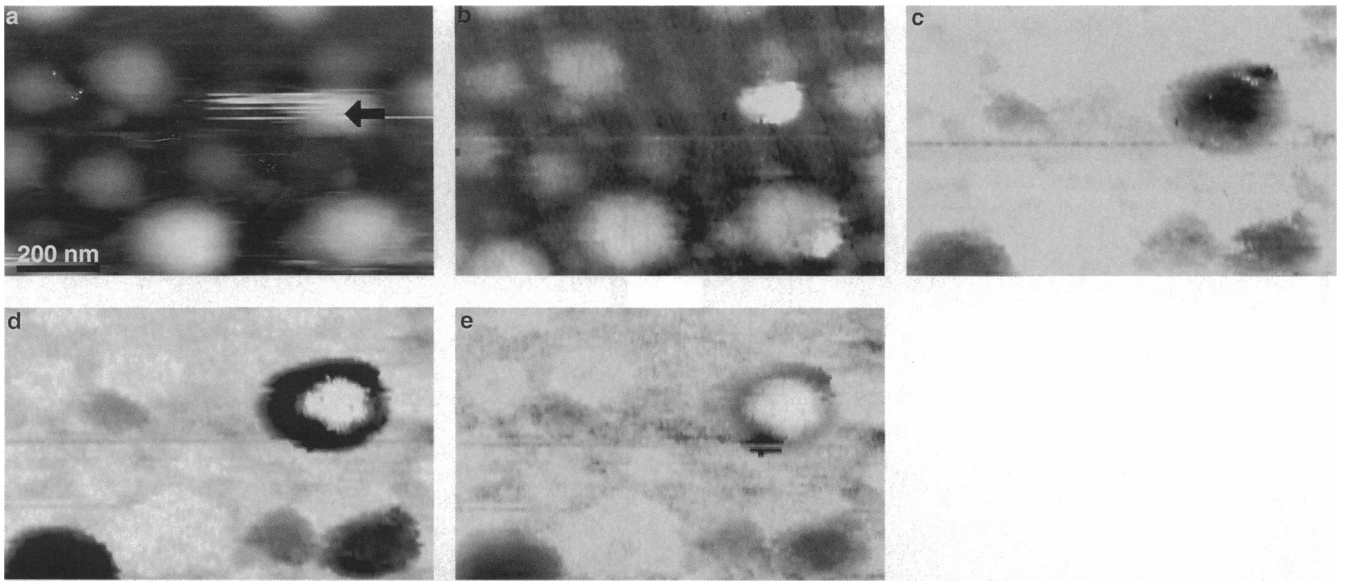

FIGURE 1 A thin nickel film (average thickness 20 nm) was evaporated onto mica. Surface tension of the nickel leads to small nickel islands exposing mica in between. (*a*) The AFM image of the sample before the force image. Note the streaks on several nickel islands (e.g., see *arrow* in *a*) that are presumably due to some contaminant. The following figures are reconstructed images out of the two-dimensional set of force curves. (*b*) The topography. (*c*) The height of the jump to contact; (*d*) the height of the hysteresis during retract; (*e*) the width of this hysteresis. For details and hints for interpretation these images, see text (image size: 1100 nm × 800 nm).

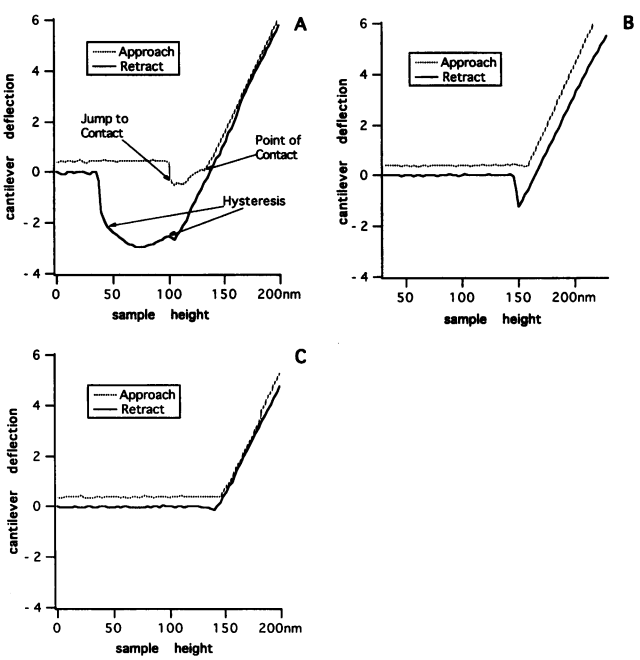

FIGURE 2 Force curves of the same sample as in Fig. 1 at different locations. Note the differences in adhesion between the contaminated nickel particle indicated by an arrow in Fig. 1 *a* (*A*), the substrate mica (*B*), and an uncontaminated nickel island (*C*). The force curves were inverted compared to Fig. 2. The tilted region in the front corresponds to the contact region, where the plateau in the back corresponds to the noncontact region of the force curves.

wetting-like hysteresis of the contaminated particle (the same that is indicated by an *arrow* in Fig. 2 *A*).

Fig. 4 shows images reconstructed out of force curves from a chromium-coated glass cover slide. Before evaporating the chromium onto the glass, a dispersion of small latex beads (450-nm diameter) was air-dried on the slide. The latex beads were removed in a sonicator after coating the sample with chromium, so that the uncovered glass was visible again. Fig. 4 *a* is the reconstructed height image, and Fig. 4 *b* the hysteresis during retract. Note that in Fig. 4 *b*, no evident difference is visible in the adhesion on the chromium (higher parts of Fig. 4 *a*) and the glass substrate. Clearly visible is that the adhesion force seems to be smaller on the boundaries between the chromium and the glass. This is probably a topographic effect (see Discussion).

Fig. 5 shows lysozyme adsorbed on freshly cleaved mica. Fig. 5 *a* is an AFM image of the sample, whereas Fig. 5, *b* and *c* show force curve reliefs recorded during lateral scanning (along the line indicated in Fig. 5 *a*). Fig. 5 *b* shows the approach trace, and Fig. 5 *c* shows the retract trace. The adhesion on the protein lysozyme is very much smaller than on the substrate. In this image, a silicon nitride tip was used.

Fig. 6 demonstrates that even single molecules can be detected through local differences in adhesion forces. Fig. 6 *a* shows the AFM image of double-stranded DNA molecules adsorbed onto mica before force curves were recorded; Fig. 6 *b* shows this after recording. Note that the multiple tip causing the image in Fig. 6 *a* disappeared after or during recording force curves resulting in a clearer image (Fig. 6 *b*). This effect of "tip cleaning" has been reported recently in a related technique of a novel tapping mode under liquids (Hansma et al., 1994). The adhesion forces, extracted out of the force curves are shown in Fig. 6, *c* and *d*, for trace and

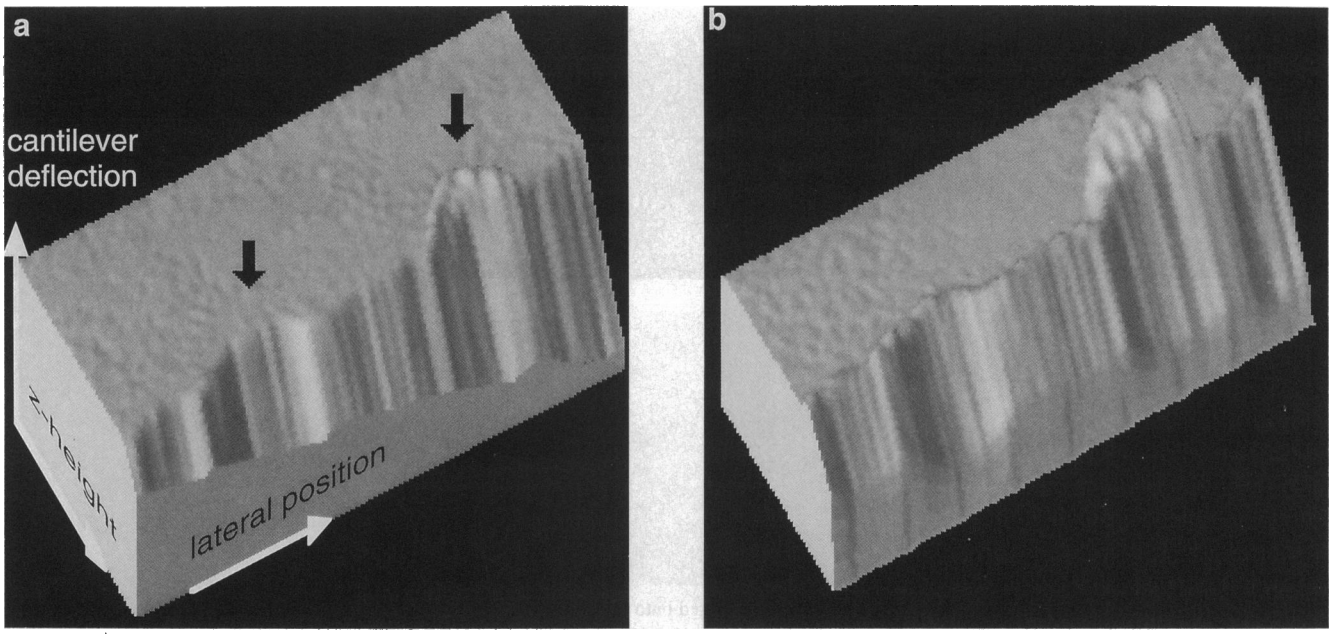

FIGURE 3 Three-dimensional reconstruction of all the force curves of one scan line containing the contaminated nickel particle indicated by an arrow in Fig. 1 *a*. The force curves are stacked one behind the other building a force relief. Two reliefs, one for the force curves measured during approach (*a*) and the other during retract (*b*) are shown. The force curves in this figure are displayed upside down compared with Fig. 2.

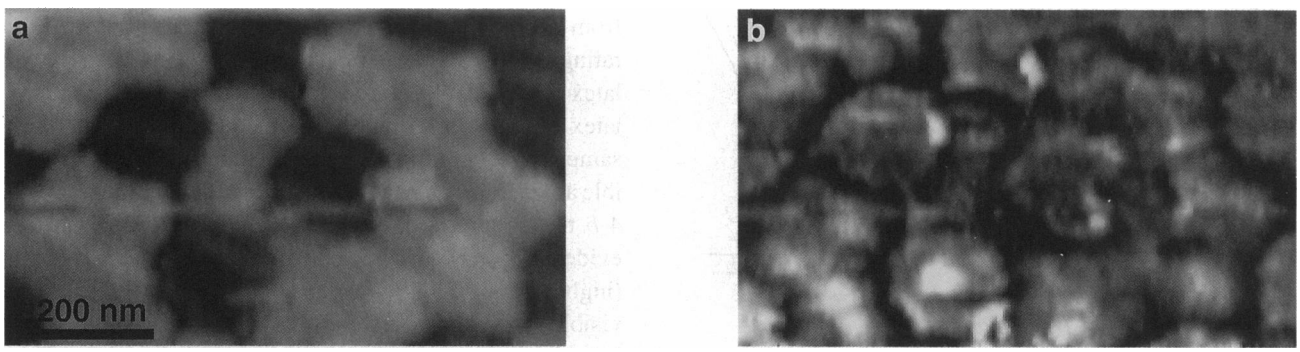

FIGURE 4 Images reconstructed from force curves from a glass slide partially coated with chromium (for details of sample preparation, see text). (*a*) The topography, the higher parts corresponding to the chromium on the glass sample. (*b*) The height of the hysteresis during retract, which is the adhesion. Note that the most prominent features in *b* are a reduced adhesion on the edges of the chromium islands (image size 1000 nm × 610 nm).

retrace, respectively. Note that the shape of the DNA is visible as a region with lower adhesion forces.

DISCUSSION

The force curve images in this paper revealed several surprising results. The adhesion forces on the metals under investigations were of the same order (chromium on glass) or even smaller (nickel on mica) than the adhesion on dielectric substrates. Because the Hamaker constants for metals are typically one order of magnitude larger than for dielectric materials (Israelachvili, 1992), the van der Waals forces also have to be larger. This fact shows that, in our case, not van der Waals forces but some other mechanism is the main source for the observed adhesion. A possible explanation is specific adhesion forces, for example, the formation of H-bonds, which has been observed in an earlier study (Hoh et al., 1992).

Another point worth discussing is the force curve shown in Fig. 2 *A*. The hysteresis during retract does not show the sharp cusp usually observed (see for instance Fig. 2, *B* or *C*), but stays approximately constant as the sample is moved farther away (see *arrows* in Fig. 2 *A*). This leads to the hypothesis that the sample stays in contact for a long distance without deflecting the cantilever further. This means that the force is only weakly dependent on the distance. This behavior is similar to the wetting force expected from a very soft and fluid-like contaminant on the sample at that spot. This contaminant might be pulled along while the tip is retracted from the surface. Because

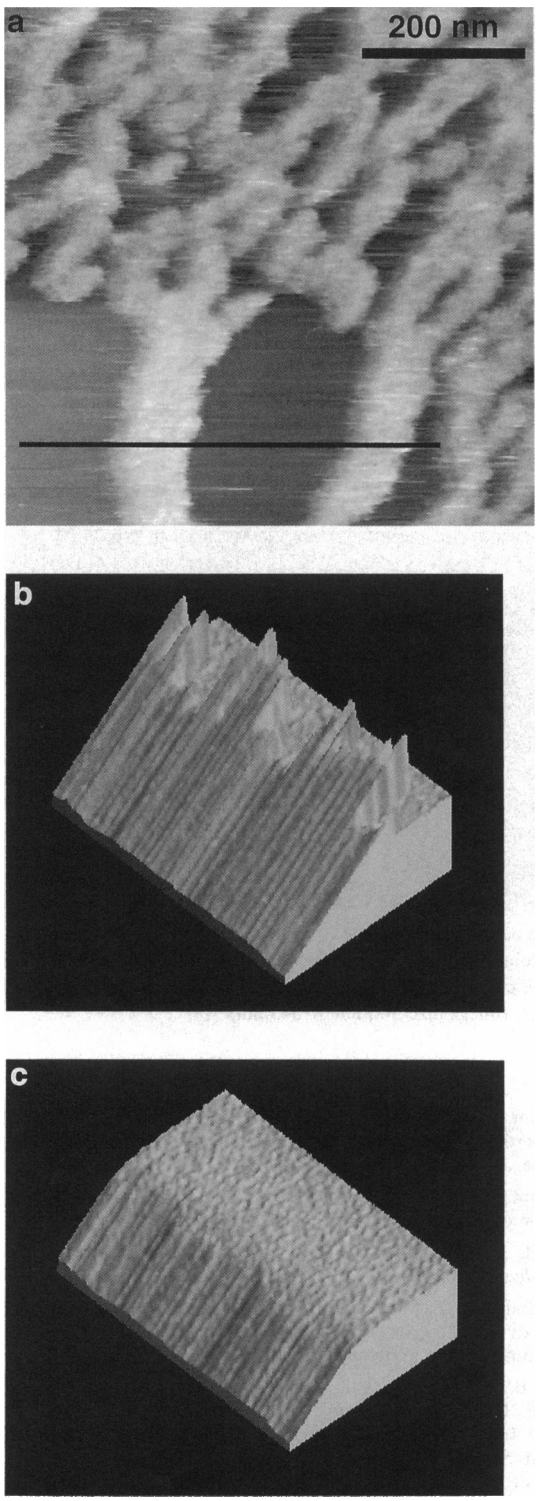

FIGURE 5 AFM image of lysozyme adsorbed on mica (*a*). The lysozyme formed aggregates on the mica, which could be imaged by AFM without destroying them. (*b*, *c*) A line of force curves recorded on the line indicated in *a*. Note that the adhesion on the substrate is much larger than on the protein (image size 700 nm × 700 nm).

the energy of this wetting is proportional to the surface area of the wetting film between tip and sample, the independence of the force with distance means that this film becomes longer, while not changing its diameter by very much. In this case, the surface energy would just be proportional to the distance, hence the force would be constant.

Fig. 4 demonstrates that some care has to be taken while interpreting forces in AFM. In this image, topography has a large effect on the forces visible. It is understandable that the contact radius between tip and sample depends on the local tilt of the sample. The point of contact of the tip will be different for different sample orientations. Knowing the geometry of the tip, one would expect the contact area be larger at the side of the tip, hence the adhesion force would be larger. Fig. 3 shows that the opposite effect can occur. This could be due to a very special tip shape, but this is unlikely because the effect of lower force appears on every side of each chromium island. This implies that the tip is relatively isotropic. Another possible explanation is that the pull off is easier because of sample tilt. The tip does not have to be pulled off in one step, but can start sliding and then be pulled off more easily. A macroscopic model is two glass slides in contact, with a thin film of water in between. It is very difficult to pull them directly out of contact, but sliding them against each other is very easy.

This is only one example showing that the geometry, especially the point of contact and local sample tilt, can have an influence on the measurable local forces. But there are many other effects possible. For instance, a very soft sample will have a much higher contact area with the tip than a hard sample (Johnson et al., 1971). Hence, the adhesion force can be higher, even if the adhesion energy per unit area is smaller. Soft, wetting contaminants on the tip can have a similar effect. One prerequisite of this technique is that the tip stays more or less unchanged during recording of the image. But it is known, from sharp tips (electron beam-deposited tips or silicon single-crystal tips (Cleveland et al., 1994)) that catastrophic events like tip breakage occur very often.

Fig. 5 shows force curve data on aggregates of lysozyme. The difference in adhesion between the lysozyme and the substrate is clearly visible: the adhesion is lower on the lysozyme than on the substrate. This demonstrates that force curve imaging works even on soft materials. This point is stressed by Fig. 6 even further, which shows images on double-stranded DNA. The resolution in this image is low: the DNA is only barely visible in the adhesion map. But the comparison of the two independent data sets acquired during trace (Fig. 6 *c*) and retrace (Fig. 6 *d*) shows clearly that single DNA molecules are detected and that the adhesion is lower on the DNA compared with the mica surface, just as for lysozyme.

CONCLUDING REMARKS

We have demonstrated that interaction forces can be imaged with molecular resolution using a novel imaging mode in AFM where force curves are recorded while the

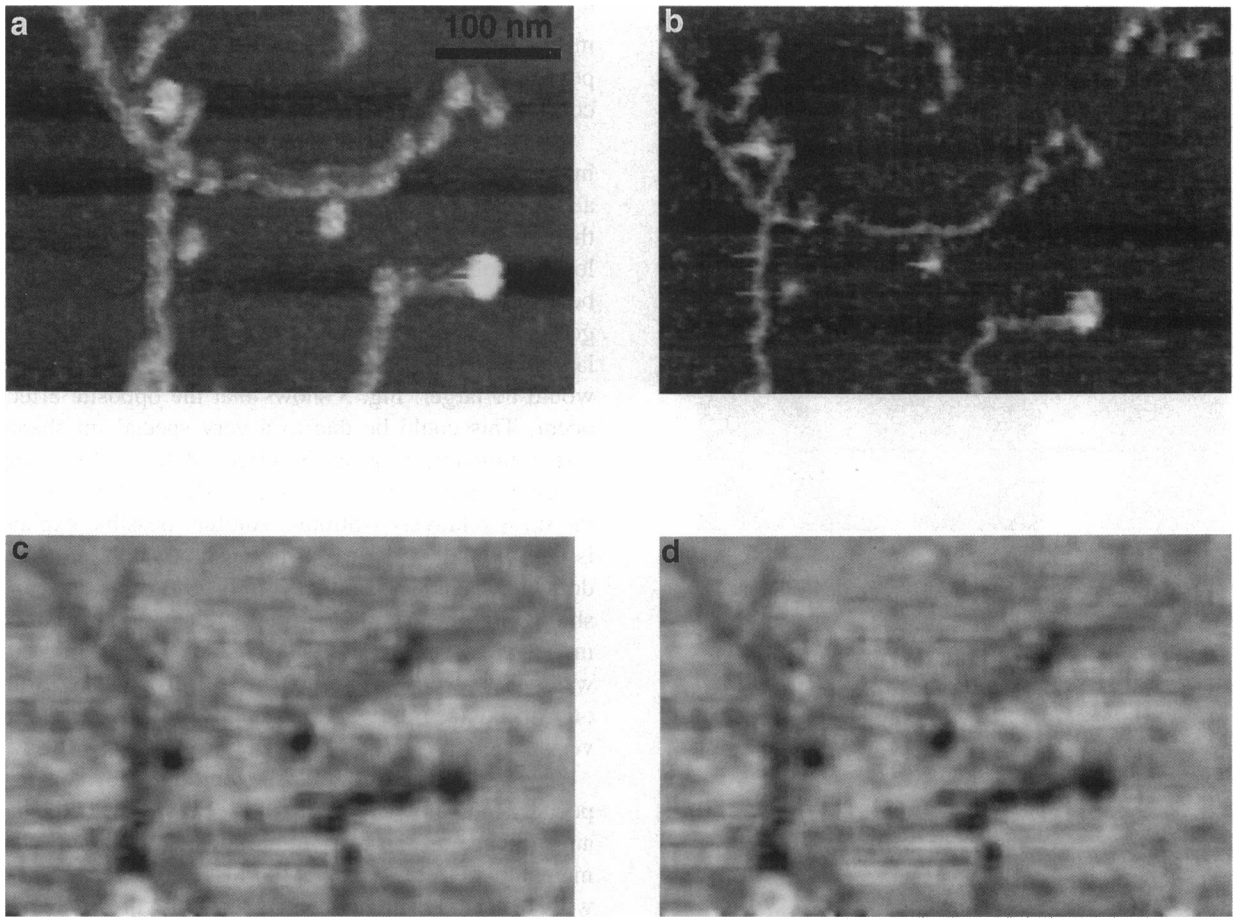

FIGURE 6 Images of several strands of DNA adsorbed on mica. (*a*) The AFM image before the force curve mapping; (*b*) after the force curve mapping. Note that the double tip apparent in *a* disappeared during force curve mapping. Therefore, the poor imaging quality of the tip in *a* might be explained by some contaminant on the tip, which was removed by recording several thousand force curves. The adhesion map calculated out of the force curve data (shown for trace *c* and retrace *d*). The DNA strands are clearly visible in these images. (image size 500 nm × 345 nm).

sample is raster-scanned under the tip. A wealth of information can be extracted out of the force curves, including topography, adhesion forces, electrostatic interactions, elasticity, and friction forces.

We thank Jan Hoh and Rainer Miehlich for helpful discussions.
This work was supported by the Office of Naval Research (M. Radmacher, J. P. Cleveland, and M. Fritz) and the National Science Foundation under awards No. DMR 9221781 (P. K. Hansma) from the Solid State Physics Program of the Division of Materials Research and DIR-9018846 (H. G. Hansma). Equipment was supplied by Digital Instruments.

REFERENCES

Akamine, S., R. C. Barrett, and C. F. Quate. 1990. Improved AFM images using microcantilevers with sharp tips. *Appl. Phys. Lett.* 57: 316–318.

Baselt, D. R., S. M. Clark, M. G. Youngquist, C. F. Spence, and J. D. Baldeschwieler. 1993. Digital signal processor control of scanned probe microscopes. *Rev. Sci. Instrum.* 64:1874–1882.

Bezanilla, M., C. Bustamante, and H. G. Hansma. 1994. Improved visualization of DNA in aqueous buffer with the atomic force microscope. *Scanning*. In press.

Binnig, G., C. F. Quate, and C. Gerber. 1986. Atomic force microscope. *Phys. Rev. Lett.* 56:930–933.

Burnham, N. A., and R. J. Colton. 1989. Measuring the nanomechanical properties and surface forces of materials using an atomic force microscope. *J. Vac. Sci. Technol.* A7:2906–2913.

Burnham, N. A., R. J. Colton, and H. M. Pollock. 1991. Interpretation issues in force microscopy. *J. Vac. Soc. Technol.* A9:2548–2556.

Butt, H. J. 1991. Electrostatic interaction in atomic force microscopy. *Biophys. J.* 60:777–785.

Cleveland, J. P., S. Manne, D. Bocek, and P. K. Hansma. 1993. A nondestructive method for determining the spring constant of cantilevers for scanning force microscopy. *Rev. Sci. Instrum.* 64:403–405.

Drake, B., C. B. Prater, A. L. Weisenhorn, S. A. C. Gould, T. R. Albrecht, C. F. Quate, D. S. Channell, H. G. Hansma, and P. K. Hansma. 1989. Imaging crystals, polymers and biological processes in water with AFM. *Science.* 243:1586–1589.

Egger, M., F. Ohnesorge, A. Weisenhorn, S. P. Heyn, B. Drake, C. B. Prater, S. A. C. Gould, P. K. Hansma, and H. E. Gaub. 1990. Wetlipid-protein membranes imaged at submolecular resolution by atomic force microscopy. *J. Struct. Biol.* 103:89–94.

Fritz, M., M. Radmacher, and H. E. Gaub. 1994a. Granula motion and membrane spreading in activated platelets imaged by AFM. *Biophys. J.* In press.

Fritz, M., M. Radmacher, N. Petersen, and H. E. Gaub. 1994b. Visualization and identification of intracellular structures by force modulation microscopy and drug induced degradation. *J. Vac. Sci. Techn.* In press.

Garnaes, G., D. K. Schwartz, R. Viswanathan, and J. A. N. Zazadinski. 1992. Domain boundaries and buckling superstructures in LB films. *Nature.* 257:508–511.

Häberle, W., J. K. H. Hörber, F. Ohnesorge, D. P. E. Smith, and G. Binnig. 1992. In situ investigations of living cells infected by viruses. *Ultramicroscopy*. 42–44:1161–1167.

Hansma, H. G., M. Bezanilla, F. Zenhausern, M. Adrian, and R. L. Sinsheimer. 1993. Atomic force microscopy of DNA in aqueous solutions. *Nucleic Acids Res.* 21:505–512.

Hansma, P. K., J. P. Cleveland, M. Radmacher, M. Bezanilla, M. Fritz, C. B. Prater, V. Elings, L. Tukunova, J. Massie, and H. G. Hansma. 1994. Tapping mode Atomic Force Microscopy in liquids. *Appl. Phys. Lett.* 64:1738–1740.

Hansma, H. G., J. Vesenka, G. Kelderman, H. Morrett, R. L. Sinsheimer, V. Elings, C. Bustamante, and P. K. Hansma. 1992. Reproducible imaging and dissection of plasmid DNA under liquid with the AFM. *Science*. 256:1180–1184.

Hartmann, U. 1991. Van der Waals interaction between sharp probe and flat samples. *Phys. Rev. B*. 43:2404–2407.

Henderson, E., P. G. Haydon, and D. S. Sakaguchi. 1992. Actin filament dynamics in living glial cells imaged by AFM. *Science*. 257: 1944–1946.

Hoh, J. H., J. P. Cleveland, C. B. Prater, J. P. Revel, and P. K. Hansma. 1992. Quantized adhesion detected with the atomic force microscope. *J. Am. Chem. Soc.* 114:4917–4918.

Hoh, J. H., and A. Engel. 1993. Friction effects in force curves. *Langmuir*. 9:3310–3312.

Hoh, J. H., R. Lal, S. A. John, J. P. Revel, and M. F. Arnsdorf. 1991. AFM and dissection of gap junctions. *Science*. 253:1405–1408.

Israelachvili, J. N. 1992. Intermolecular and Surface Forces. Academic Press, London.

Johnson, K. L., K. Kendall, and A. D. Roberts. 1971. Surface energy and the contact of elastic solids. *Proc. R. Soc. London Ser. A*. 324: 301–313.

Keller, D., L. Chang, K. Luo, S. Singh, and M. Yorganciogla. 1992. Scanning force microscopy of cells and membrane proteins. *Proc. SPIE*. 1639: 91–101.

Keller, D., and C. Chih-Chung. 1992. Imaging steep, high structures by scanning force microscopy with electron-beam deposited tips. *Surf. Sci.* 268:333–339.

Marti, O., J. Colchero, and J. Mlynek. 1990. Combined scanning force and friction force of mica. *Nanotechnology*. 1:141–144.

Mizes, H. A., K.-G. Loh, R. J. D. Miller, S. K. Ahuja, and E. F. Grabowski. 1991. Submicron probe of polymer adhesion with atomic force microscopy: dependence on topography and material inhomogeneities. *Appl. Phys. Lett.* 59:2901–2903.

Ohnesorge, F., and G. Binnig. 1993. True atomic resolution by AFM. *Science*. 260:1451–1456.

Radmacher, M., M. Fritz, J. P. Cleveland, D. R. Walters, and P. K. Hansma. 1994. Characterization of lysozyme adsorbed on glass by Atomic Force Microscopy. *Langmuir*. In press.

Radmacher, M., R. W. Tillmann, M. Fritz, and H. E. Gaub. 1992. From molecules to cells—imaging soft samples with the AFM. *Science*. 257: 1900–1905.

Radmacher, M., R. W. Tillman, and H. E. Gaub. 1993. Imaging Viscoelasticity by Force Modulation with the Atomic Force Microscope. *Biophys. J.* 64:735–742.

Rugar, D., and P. K. Hansma. 1990. Atomic Force Microscopy. *Physics Today*. 23–30.

Tao, N. J., N. M. Lindsay, and S. Lees. 1992. Measuring the microelastic properties of biological materials. *Biophys. J.* 63:1165–1169.

Weisenhorn, A. L., P. K. Hansma, T. R. Albrecht, and C. F. Quate. 1989. Forces in atomic force microscopy in air and water. *Appl. Phys. Lett.* 54:2651–2653.

Weisenhorn, A. L., M. Khorsandi, S. Kasas, V. Gotozos, M. R. Celio, and H. J. Butt. 1993. Deformation and height anomaly of soft surfaces studied with the AFM. *Nanotechnology*. 4:106–113.

Weisenhorn, A. L., P. Maivald, H.-J. Butt, and P. K. Hansma. 1992. Measuring adhesion, attraction, and repulsion between surfaces in liquids with an atomic force microscope. *Phys. Rev. B (Condensed Matter)*. 45: 11226–11232.